

The Effects of a New Grain Boundary Phase in Ni-Al Alloy

Y.L. Chiu, A.H.W. Ngan and I.P. Jones*

Department of Mechanical Engineering, The University of Hong Kong, Pokfulam Road, Hong Kong, P.R.China; * School of Metallurgy and Materials, University of Birmingham, Edgbaston, B15 2TT, England.

ABSTRACT

In a γ/γ' nickel-aluminum alloy, a new phase has been identified along grain boundaries by conventional transmission electron microscopy. This phase is identified to be of the C_6Cr_{23} type structure with lattice parameter 10.48\AA , which is approximately three times that of Ni_3Al or nickel. This grain boundary precipitate is found to be coherent with the γ phase in one grain. The chemical composition of this grain boundary precipitate is determined by energy dispersive x-ray spectroscopy and parallel electron energy loss spectroscopy. The deformation mechanism of this grain boundary precipitate is investigated on post-mortem specimens which have been carefully deformed by nanoindentation after jet-polishing.

INTRODUCTION

It is well-known that a tiny addition of boron can significantly improve the ductility of nickel-rich Ni_3Al alloys [1-3]. Recently, the effects of boron additions on the mechanical properties and microstructure of γ/γ' two-phase alloys have been investigated [4-5]. The ductility and impact toughness of the two-phase alloys were found to be significantly improved upon boron addition. On the other hand, the work hardening rate and grain growth rate were decreased by very small amounts of boron doping. Investigation of the grain boundary chemistry and the structure of γ/γ' alloy, therefore, becomes critical for a thorough understanding of the mechanical behaviors. In this paper, some observations on the chemistry and microstructure of a γ/γ' nickel aluminum alloy are presented. The effects of grain boundaries in hindering plastic deformation are evaluated by localized nanoindentation near grain boundaries in jet-polished thin foils.

EXPERIMENTAL

The material used was a γ/γ' nickel-aluminum alloy with about 85 at.% nickel, 0.5at.% boron with the balanced aluminium. The preparation method has been described in an earlier report [4]. The alloy was homogenized at 1373K for 48 hours in vacuum. Thin foils suitable for transmission electron microscope (TEM) observation were prepared by electropolishing using perchloric acid in methanol. Chemical information at the grain boundaries was obtained by X-ray energy dispersive spectroscopy analysis (EDX) and parallel electron energy loss spectroscopy (PEELS) on a Tecnai F20 FEG-TEM operating at 200 kV. In order to evaluate the role of grain boundaries during plastic deformation, nanoindentation was performed on jet-polished thin foils supported by wax. The nanoindentation was performed using a Hysitron system, where small loading down to the μN range could be applied through a Berkovich indenter (fig.1). After deformation, the foils were cleaned by immersing in ethanol to dissolve the wax.

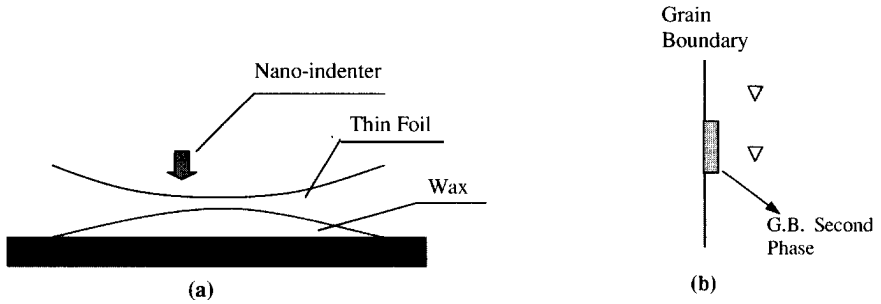


Figure 1. (a) Schematic showing localized deformation of a TEM thin foil by nanoindentation. (b) Plan view showing the indentations near a grain boundary

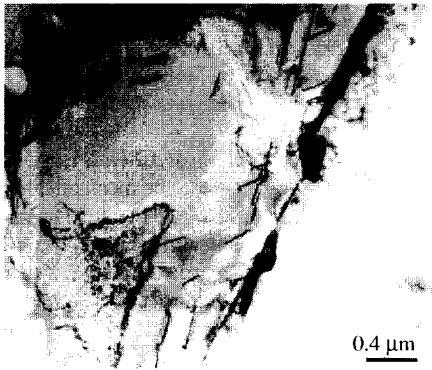


Figure 2. Micrograph showing the grain boundary phase. The precipitates are about 0.1–0.2 μm wide and discontinuously decorates the grain boundary.

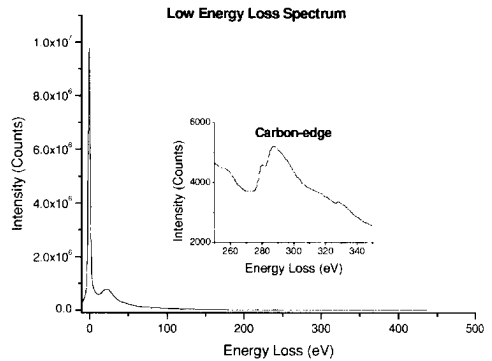


Figure 3. Low energy loss spectrum showing carbon is the only detectable light element in the compound.

RESULTS

Fig. 2 shows precipitates of the grain boundary phase in the alloy after homogenization. These are about 100nm wide and 2 μm long. The crystallographic structure of this grain boundary phase was determined by electron diffraction techniques. Fig. 4 shows the selected area diffraction patterns taken from the $\text{L1}_2 \text{Ni}_3\text{Al}$ phase near the grain boundary phase and those taken from the grain boundary phase under the same incident beam conditions. It is noted that the grain boundary phase possesses a face-centred-cubic structure. The lattice parameter is about three times of that of Ni_3Al . Therefore, the crystal structure of this grain boundary phase is the Cr_{23}C_6 type. In all the specimens checked, we found that this phase is always associated with γ - γ

boundaries. The grain boundary phase is always coherent with the γ' rather than the γ matrix, and no interfacial dislocations could be observed.

EDX measurements of this grain boundary phase indicate a composition of 61.5% nickel, 6.4% aluminum and 32.1% carbon. PEELS was also used to make sure there were no other light elements in the compound. The low energy loss spectrum in fig. 3 shows that only the carbon-edge is observable and no other light elements, especially boron, could be found. This grain boundary compound, therefore, can be identified as a Ni-Al-C ternary carbide.

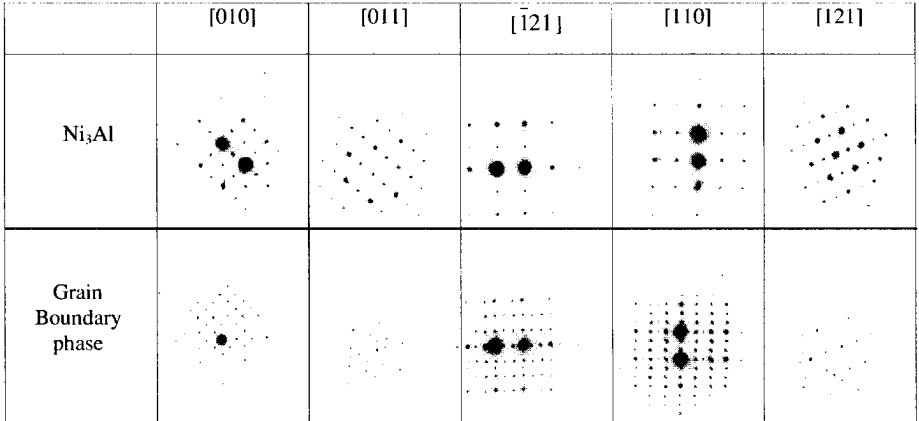


Fig. 4 Diffraction patterns from Ni₃Al and the grain boundary phase under different beam directions.

Fig. 5(a) shows a grain boundary free from carbide. After the localized deformation of the γ' phase by nanoindentation, screw superdislocations with a $[\bar{1}10]$ Burgers vector were pushed outward from the indent region on octahedral planes, the $(11\bar{1})$ plane in this case. The parallel lines, indicated by arrows in fig. 5(b), are slip traces on the specimen surface. The dislocations can be seen to bow-out away from the indent. All these slip traces, however, terminate at a grain boundary. Upon approaching the grain boundary, the hitherto screw dislocations re-orientated their line direction onto the grain boundary plane, as shown in fig. 5(c) when the grain boundary is tilted edge-on. Another point that is worth noting is that some points of the grain boundary, as shown by the dotted arrows in fig. 5(b-c), zigzag at the head of these dense slip bands.

Fig. 6(a) shows a grain boundary decorated with a carbide phase about 200nm wide and distributed discontinuously along the grain boundary. The crystallographic orientation of the carbide is the same as the grain on the right. The indent is again on the γ' phase side of the grain boundary and is located near the lower right corner of the micrograph. Long screw superdislocations with Burgers vector $[0\bar{1}1]$ are dominant in the foil. Parallel to those long screw dislocations are dense APB tubes which show discernible contrast when the diffraction vector is perpendicular to them (fig. 6(c)), but are out of contrast when the diffraction vector is parallel (fig. 6(d)) [6]. Similar APB tubes were also observed in some grain boundary regions without the

carbide phase, and so their occurrence may not be related to the carbide phase. It is also noted that in the left grain in fig. 6, few dislocations could be found to emanate from the particular grain boundary decorated with carbide; most of the observed dislocations are from the portions free from carbide (fig. 6(e)).

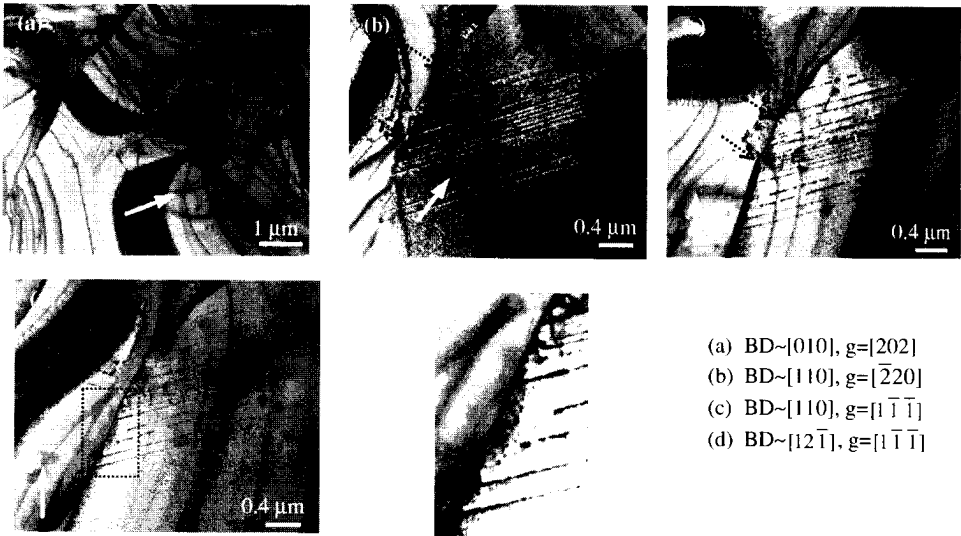


Figure 5. Micrographs showing that nanoindentation induced dislocations moving on slip bands, pile-up or terminate at a grain boundary. Some dislocations adjust their line direction to be parallel with the grain boundary plane, as shown in (d) where the lower part of the grain boundary is tilted to be edge on. The dashed square is magnified in (e). Grain boundary sliding seems to be triggered at several points under intensive shearing as shown by the dotted arrows in (b-c).

DISCUSSION

It is well-known that metallic elements may form various carbides in the form of M_xC_y in nickel-base superalloys [7,8], among which $M_{23}C_6$ has drawn most attention due to its beneficial effects on creep life [7]. $M_{23}C_6$ has a complex cubic structure with a lattice parameter about 10.5\AA , which is a near multiple of the lattice parameter of γ/γ' . The electron diffraction patterns in Table I confirm the $M_{23}C_6$ structure of the grain boundary carbide in the present investigation. It is interesting to note, however, that according to EDX measurements, the compound should have the composition $Ni_{62}Al_6C_{32}$. This composition is similar to that of another carbide (M_7C_3), albeit M_7C_3 has a hexagonal structure. The possibility of other elements in this compound is ruled out by the PEELS results, which indicate that carbon is the only light element observable within the low energy-loss regime. According to the authors' knowledge, there are only two known Ni-Al-C ternary compounds, namely, Ni_3AlC and $Ni_{69}Al_{23}C_8$, but both have a unit size less than 4\AA . Therefore, this grain boundary carbide is a new Ni-Al-C ternary compound possessing the $M_{23}C_6$ structure.

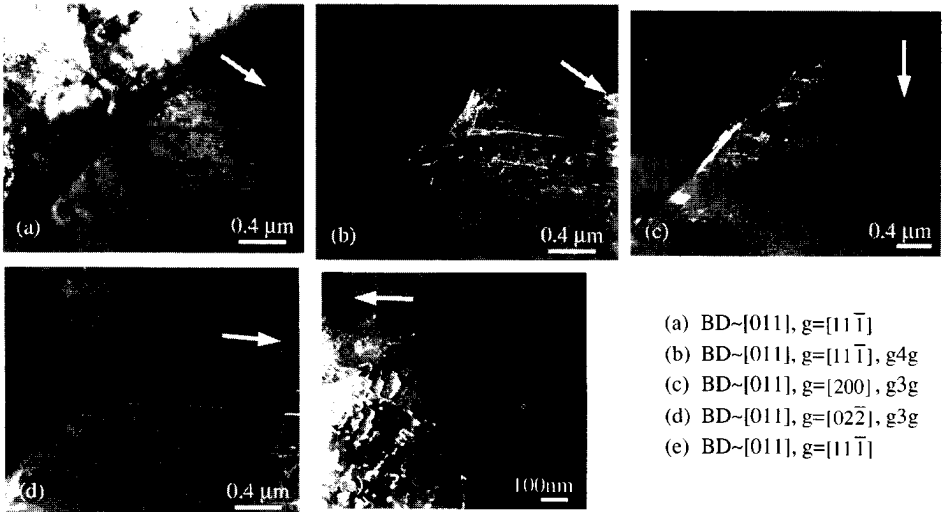


Figure 6. TEM micrographs showing (a) carbides along a grain boundary and long dislocations, (b) very dense APB tubes parallel to the long dislocations, (c) long dislocations out of contrast with the APB tubes in contrast, (d) APB tubes out of contrast when g is parallel to them, (e) to the left of the grain boundary, fewer nucleated dislocations can be observed where there is carbide (the upper part of the grain boundary).

Recent work by Bor et al. [9] demonstrated that the morphology and structure of carbide in superalloys could be modified by small amounts of dopants and the creep performance could be optimized by discontinuous grain boundary $M_{23}C_6$. As the creep life is usually determined by the ease of strain relief at the grain boundaries, any factor hindering grain boundary sliding and cavity nucleation becomes beneficial to high temperature applications. In the present study, the relief of strain accumulation at grain boundaries differs somehow with and without the grain boundary carbide. As shown in fig.4, when dislocations approach a carbide-free grain boundary under an applied stress, they re-align along the grain boundary plane, where a higher mobility of dislocations is expected. Thus the stress pile-up at the grain boundaries, as implied by the slip band popularity, can be effectively relieved. In this way, the grain boundary might be tilted or sheared considerably as grain boundary dislocations sweep out. Fig. 5(b) shows such a scenario. With the presence of carbide at a grain boundary, as shown in fig. 6, dislocations originating from the γ' phase could not reach the grain boundary due to the blockage by the coherent carbide. Hence, the carbide decorated portion of the grain boundary could stand very severe strain accumulation before shearing occurs at the tips of slip bands. Considering the coherency between the carbide and γ' , the interface between them might be expected to be of low energy and thus strong. The role of the carbide is like a strain-free buffer to the grain boundary, so that the accumulated stress on the undeformed side of the grain boundary due to dislocation pile-up on the deformed side of the grain boundary would be lower than the situation without the

carbide. The observed lower density of nucleated dislocations in the undeformed grain whenever a carbide particle is present reflects this.

CONCLUSIONS

In a TEM study of a boron-doped γ/γ' nickel-aluminum alloy, a new carbide at the grain boundaries was identified to have the $M_{23}C_6$ cubic structure with a lattice parameter of about 10.5Å, i.e., around three times of that of the γ or γ' phases. The chemical composition was analyzed to comprise nickel (61.5 at.%), aluminum (6.4 at.%) and carbon (32.1 at.%). In the absence of carbide, screw dislocations approaching a grain boundary are able to re-align themselves onto the grain boundary plane to relieve the stress concentration ahead of the slip band, but the grain boundary becomes twisted at some positions. When the grain boundary is decorated with carbide particles, no grain boundary shearing has been observed in the present study. The cohesive strength of the grain boundary decorated by this carbide phase could be expected to be no less than that without carbide, i.e., this carbide containing alloy might provide better creep properties.

ACKNOWLEDGMENT

This research was carried out under financial support from the Hong Kong Research Grants Council (Project no. HKU 7078/98E). YLC would like to thank the Royal Society for supporting a study visit to the University of Birmingham.

REFERENCES

1. K. Aoki, O. Izumi, *J. Jap. Inst. Metals*, **43**, 1190 (1979).
2. C. T. Liu, C. L. White, J. A. Horton, *Acta Metall.*, **33**, 213 (1985).
3. E. M. Schulson, T. P. Weihs, I. Baker, H. J. Frost and J. A. Horton, *Acta Metall.*, **34**, 1395 (1986).
4. Y.L. Chiu and A.H.W. Ngan, *Scripta Mater.*, **40**, 27 (1999).
5. Y.L. Chiu and A.H.W. Ngan, *Met. Mater. Trans.*, (in press)
6. A.H.W. Ngan, I.P. Jones and R.E. Smallman, *Phil. Mag. B*, **67**, 417 (1993).
7. H.E. Gresham, *Met. Mater.*, **3**, 433 (1969).
8. R.T. Holt and W. Wallace, *Int. Met. Rev.*, **203**, 1 (1976).
9. H.Y. Bor, C.G. Chao and C.Y. Ma, *Met. Mater. Trans.*, **31A**, 1365 (2000).